Dielectric Relaxation Studies of Annealed Short Side Chain Perfluorosulfonate Ionomers

Shunfua Su and Kenneth A. Mauritz*

Department of Polymer Science, University of Southern Mississippi, Southern Station Box 10076, Hattiesburg, Mississippi 39406-0076

Received July 22, 1993; Revised Manuscript Received January 10, 1994®

ABSTRACT: Annealing of dry, short side chain Na^+-perfluorosulfonate ionomers at a submelting temperature above the ionic cluster glass transition results in increased order and more structural cohesion in the matrix and disruption of order in the clusters as seen by DSC. Hydrative capacity increases with increased annealing. Electrical impedance studies show how the permittivity representation of data is most useful for studying long-range ion motions while admittance is better suited for detecting cluster-confined motions. A cluster-associated peak was rationalized as shifting to lower frequencies with increase in temperature/time of annealing due to an increase in hydrated cluster size. Analysis of the distribution of relaxation times indicates that annealing above the cluster glass transition induces considerable microstructural regularity within these membranes. Permittivity/admittance spectra of "dry" and hydrated membranes suggest that annealing induces ion-hopping pathways that are rather tortuous. It is proposed that, while side chain packing within clusters becomes disordered upon annealing, the semicrystalline matrix surrounding clusters becomes more homogeneous and tightly packed, thereby blocking intercluster ion hopping to a greater degree.

Introduction

Annealing of polymers often modifies their physical properties. When glassy polymers are annealed, free volume relaxation and increased brittleness occur. T_g can increase while the glass transition breadth decreases, indicating a decrease in microstructural heterogeneity. The degree of crystallinity in semicrystalline polymers can increase with submelting annealing owing to increase in chain packing order within crystallites and/or incorporation of more stereoregular chain segments into crystallites. Annealing below T_g imparts additional thermal kinetic energy to chain segments allowing them to seek out more efficient packing. Following annealing, the polymer is closer to a true equilibrium state. Annealing above T_g followed by rapid cooling to a glassy state freezes in more free volume than existed in the original glassy state.

Perfluorosulfonate ionomers (PFSIs), in addition to having crystalline and amorphous regions associated with the packing of short $(CF_2)_x$ chain sections, have ionic side chains that aggregate to form *clusters* that are nanometers in size.[1] In consideration of the annealing of these complex nanophase-separated systems, a modification of the packing of the side chains should also be considered. The sulfonate-terminated side chains may loosely interdigitate in rough radial fashion as inverted surfactant micelles. It is quite reasonable to expect that annealing-induced structural rearrangements within the crystalline + amorphous backbone – associated regions are *coupled* to structural changes within the clusters by virtue of covalent linkages. It is reasonable to think that the degrees of packing order for the phases are somehow inversely related in that a high degree of order within one phase is achieved at the expense of disrupting order in another coupled phase.

In this work, short side chain (SS) PFSI membranes of a single equivalent weight (EW = 803 g/equiv of resin) that were supplied by Dow Chemical Co. were analyzed in the Na^+ ion form either dry or highly hydrated.

Thermal transitions were studied using differential scanning calorimetry (DSC) for membranes annealed either for a fixed time at different temperatures or at a fixed temperature for different times. Long times might cause the same structural modification as high temperatures; waiting long enough at a "low" fixed temperature, the same structural relaxation might eventually be effected as that achieved at a higher temperature but for shorter time. Finally, the temperature of annealing relative to temperatures of various thermal transitions is a critical factor.

We reported dielectric relaxation (DR) studies of SS PFSIs having various hydration levels[2] or as imbibed with aqueous H_2SO_4 of various concentrations.[3] The major goal of the work in this paper was to investigate the DR response of dry and hydrated Na^+-form membranes annealed for various times and temperatures. If annealing affects molecular packing, it will also generate DR spectra different from spectra for corresponding unannealed membranes.

Experimental Section

Membrane Initialization. SS PFSI membranes of 803 EW with nominal thickness of 0.085 mm were supplied by Dow Chemical Co. All as-received films were initialized to the same standard state according to the following procedure before annealing and, in some cases, then hydrated.

The membranes were equilibrated in 14 M aqueous NaOH solutions 48 h at 22 °C to effect total replacement of existing ions on sulfonate groups with Na^+ ions. Then the films were soaked in deionized water for 48 h to leach out excess Na^+ and associated OH^- ions. High-purity deionized water was obtained by circulating house distilled water through a Nanopure water purification system. This leaching creates the mole ratio SO_3^-:Na^+ = 1:1 and considerable hydration within the membrane. Samples were then surface-blotted dry and placed on glass plates which were transferred to a vacuum oven and dried for 48 h at 22 °C to remove loosely bound water. As inferred later, residual water still remains within the membranes. Samples were then punched into circles 1.0 in. in diameter for DR analysis and stored in a desiccator at room temperature for future use. Owing to the fact that the properties of PFSIs are affected by sample prehistory, all membranes were initialized in *exactly* the same fashion.

Annealing. Some initialized membranes were placed in a vacuum oven and annealed (without vacuum) at 110 °C for 2 days. Other membranes were placed in a high-temperature oven (no vacuum) at 295 °C for time periods from 1 h to 2 days. The reason for annealing at the high temperature of 295 °C is explained

® Abstract published in *Advance ACS Abstracts*, March 1, 1994.

0024-9297/94/2227-2079$04.50/0

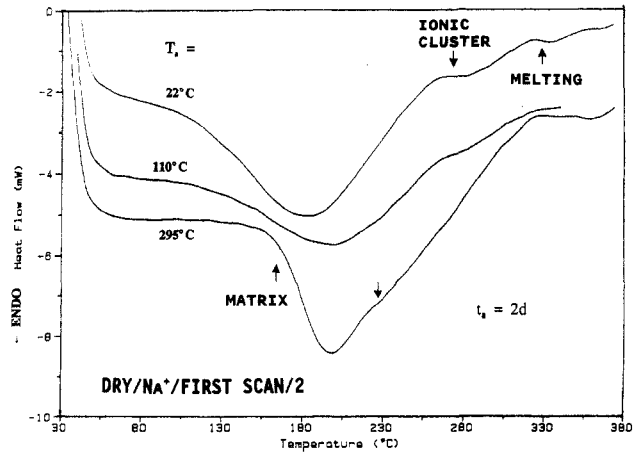

Figure 1. First-scan DSC thermograms from 30 °C to beyond crystallite melting for dry Na^+-form, short side chain, 803 EW PFSI membranes annealed at 22, 110, and 295 °C for 2 days.

in the discussion of the DSC results which indicated that 295 °C is above a thermal transition. After annealing, the membranes were cooled to room temperature over a period of ~6 h and again dried under vacuum at room temperature for 2 days to remove moisture that might have been absorbed from the atmosphere during cooling. After this, the samples were stored in a desiccator until used.

Differential Scanning Calorimetry. Thermograms were obtained/analyzed using a DuPont Model 910 DSC module with a Model 9900 computer. Scans were made on samples of ~20 mg over a temperature range 30–350 °C. The heating rate was 20 °C/min for membranes annealed at different temperatures for fixed 2-day periods and 40 °C/min for membranes annealed at the same temperature for different times.

Equilibrium Water Uptake. Dry initialized and annealed membrane samples were soaked in deionized water at 22 °C for 6 days. This time is more than sufficient to achieve "equilibrium" swelling. After blotting surface-attached water, the weight percent of water uptake relative to the dry weight was determined.

Dielectric Relaxation Measurements. Treated membranes were placed between two flat parallel stainless steel electrodes sealed within two stainless steel cups. The electrodes are insulated from the cups. Owing to the fact that the electrodes are in intimate, pressed contact with the membrane, it is difficult for water vapor to enter/escape from the sample except at the thin edge of the circle. To prevent transfer of water vapor across the edge, a circular Teflon block was introduced between the upper cup and lower electrode. It is difficult for water vapor to enter/escape from this small sealed compartment. During the time when impedance data are collected for a dry membrane, water vapor will not enter the sample from the atmosphere, or for a highly hydrated membrane, water vapor will not escape to the atmosphere.

A Hewlett-Packard 4192A LF impedance analyzer was used to obtain the complex impedance (Z^*) and complex admittance (Y^*) over the frequency (f) range 5 Hz to 13 MHz for an applied low-amplitude sinusoidal signal. The complex permittivity (ϵ^*) was derived from Z^* in a way described in an earlier report.[3] While an equivalent electrical circuit for the ionomer will be discussed, the displayed graphs of the real and imaginary components of Y^* and ϵ^* are independent of an assumed arrangement of resistors, capacitors, and Warburg (diffusional) elements. All dielectric relaxation experiments were performed at constant room temperature (22 °C).

After impedance measurements were taken for the dry samples, the membranes were soaked in deionized water at 22 °C. After 2 days, the membranes were removed, surface-blotted dry, and rapidly sandwiched between the two electrodes and the electrical measurements repeated.

Results and Discussion

Variation of Temperature of Annealing. Differential Scanning Calorimetry. In Figure 1 are first-scan DSC thermograms, from 30 °C to above the established TFE crystallite melting temperature, for membranes annealed at 22, 110, and 295 °C for 2 days.

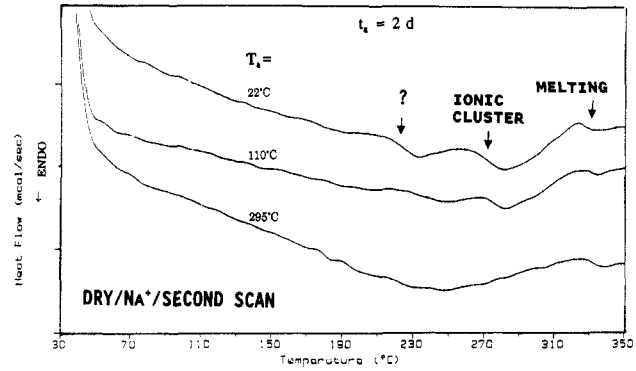

Figure 2. Second-scan DSC thermograms as in Figure 1 except for samples quenched from 210 °C immediately after end of first DSC run.

Table 1. DSC Thermal Transition Temperatures[a] (°C) for 803 EW Short Side Chain, Dry Na^+-Form PFSI Membranes[b]

T_a	$T_{g,m}$	$T_{g,c}$	T_m
22	215	282	332
110	230	282	335
295	240		338

[a] Listed temperature of a transition refers to the inflection point. While temperatures in the second column are labeled $T_{g,m}$, there is question as to whether they are matrix related. [b] Samples were annealed for 2 days at the three indicated temperatures (T_a). Data are for the second scan at 20 °C/min.

Moore and Martin detected a weak DSC transition in first scans at ~179 °C for an 803 EW short side chain Na^+-form PFSI, referred to as a "matrix glass transition" ($T_{g,m}$).[4] This transition is also present in our samples in the first scan. It is seen that $T_{g,m}$ shifts to higher temperatures with increased temperature of annealing (T_a). The endotherm for T_a = 295 °C is considerably more profound than those for the unannealed (22 °C) and 110 °C annealed membranes. This result is quite reproducible. Perhaps annealing at 295 °C induces more order or structural cohesion in the perfluorocarbon regions. It is also noted that the *width* of this transition is considerably narrower for T_a = 295 °C, suggesting that the *degree of microstructural heterogeneity* in the matrix decreases.

Tant *et al.* performed a dynamic mechanical analysis (DMA) of 800 EW Na^+-form SS PFSIs.[5] Oddly, the matrix glass transition of Moore and Martin, also seen in our work, is not detected in this DMA study.

Seen in Figure 1 is a $>T_{g,m}$ and submelting transition which is pronounced for T_a = 22 °C, weaker for 110 °C, and not visible for 295 °C.

Another sample from the same membrane was heated in the DSC to only 210 °C (just above $T_{g,m}$) in like fashion and then rapidly cooled using ice. These samples experienced neither the cluster transition nor melting. This quenching was immediately followed by second scans from 30 to 350 °C for each T_a, seen in Figure 2. On inspection of Figure 2, the matrix glass transition is *apparently* suppressed for T_a = 22 and 110 °C. (It might be argued that a vestige is present on the 295 °C curve, which is reasonable considering that this event was most profound for T_a = 295 °C on the first scan.)

There are three features on the scans in Figure 2 for which approximate temperatures are in Table 1.

(1) There is a strong endotherm at ~215 °C for the unannealed (22 °C) sample which is weak for annealed samples. The transition temperature increases to 240 °C

at T_a = 295 °C. This feature is absent in first scans, although a slight inflection is seen just below 230 °C for T_a = 295 °C (Figure 1). Evidently, the first heating is responsible for its appearance. Neither Moore and Martin nor Tant *et al.* report this transition. While it is tempting to think this is the matrix glass transition elevated to higher temperatures by prior "dynamic annealing", the rapid quench applied at the end of the first scan would freeze in molecular disorder accumulated up to 215 °C so as to erase this transition.

(2) A pronounced transition at ~282 °C is present on second scans for the unannealed and 110 °C annealed membranes but absent on the T_a = 295 °C scan. This transition is also seen for T_a = 22 and 110 °C but not for 295 °C on first scans. In either first or second scan, the transition magnitude diminishes with increasing T_a. Moore and Martin[4] also detected an endothermic transition at the same temperature, which was referred to as an "ionic cluster glass transition temperature" ($T_{g,c}$). If this relaxation involves the onset of ionic side chain mobility, annealing at $T_a > T_{g,c}$, followed by rapid cooling, will freeze in side chain packing *disorder*. An *order* → *disorder* transition is unable to occur upon reheating because disorder already exists in clusters. Loose side chain packing will result in more free volume within clusters so that they can become more hydrated.

(3) The endotherm associated with melting PTFE-like crystallites is seen (~332–338 °C for the second scan, Table 1) for unannealed as well as annealed membranes. Moore and Martin reported T_m = 335 °C for 803 EW SS PFSI films.[4] The upward shift in T_m (Table 1) with increased T_a is attributed to perfection of microcrystalline order induced by enhanced thermal molecular motions along the backbone.

Water Sorption. The equilibrium water uptakes for the membranes are 22.6% (22 °C), 23.7% (110 °C), and 27.4% (295 °C). Membrane hydration capacity *increases* with increasing T_a at constant time of annealing = t_a.

Consider T_a trends in first DSC scans that correlate with T_a trends in water sorption. It was seen that the matrix glass transition for T_a = 295 °C is more profound than that for both unannealed and 110 °C annealed membranes. Also, the difference between water uptake for T_a = 295 and 110 °C is a bit greater than the difference between T_a = 110 and 22 °C. The cluster glass transition becomes weaker with increased T_a. Perhaps annealing induces more order in the matrix while disrupting order in the clusters because the two phases are covalently *coupled*. Considering the trends in the matrix and cluster glass transitions, it might be thought that, as clusters become more disordered upon annealing, incorporated side chains pack less efficiently, thereby creating more free volume in the ionic regions. This increased cluster free volume, coupled with the fact that water preferentially resides in clusters, might account for the increase in water uptake with increased T_a.

An alternate explanation for the water uptake *vs* T_a trend consists of rationalizing that clusters grow in size with annealing. Not all charged side chains are expected to pack neatly into clusters, some being trapped in isolation during processing since film formation is a kinetic process. This is plausible especially if side chains are distributed randomly along the backbone as stated by Tant *et al.*[5] The broadness of the SAXS "cluster peak" observed for PFSIs suggests that the degree of intercluster order is not high.[4]

Increased mobility of chain segments and side chains imparted through annealing would coax isolated side chains into a more energetically favorable state within clusters and/or cause smaller clusters to coalesce into larger clusters. "Cluster coalescence" is favorable through reducing polar/nonpolar interfacial tension (*i.e.*, reducing cluster surface/volume ratio). Thus, by affecting larger ionic domains, equilibrium water uptake is enhanced. If microphase separation is improved thusly, enhancement of the cluster glass transition magnitude should be observed; in fact, the opposite occurs with increasing T_a.

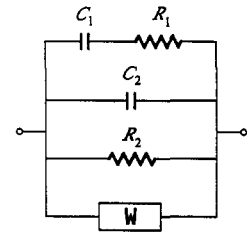

Figure 3. Equivalent impedance circuit representation for PFSI membranes.

Dielectric Relaxation. Equivalent Circuit. The equivalent circuit in Figure 3 is reasonable for PFSI membranes,[3] though only accounting for the main features on the ϵ' and ϵ'' *vs* ω curves. Resistor R_2 and Warburg element W represent long-range (intercluster) ion displacements due to *drift* and *diffusion*, respectively, at low frequencies. W, a complex quantity having real and imaginary parts of equal magnitude, is proportional to $f^{-1/2}$ and $D_i^{-1/2}$, D_i being the diffusion coefficient of ion i.[6] While partitioning intercluster ion hopping into pure drift (ohmic) and diffusion terms can be questioned, it is often performed in the analysis of electrochemical processes.[6] R_1 represents oscillatory *intra*cluster ion motions and C_1 the capacitance resulting from charge separation across clusters. The accumulation of ionic charge at cluster boundaries is detected during the first and third quarters of applied electric field oscillation.[7] Charge accumulates at cluster boundaries because of an ionic mobility gradient across the interfaces. The separation of considerable ionic charge across a few nanometers generates a large dipole moment per cluster which discharges during the second and fourth quarters if the period is on the order of the time scale of relaxation of interfacial polarization.

It was suggested that a *fractal model* is more realistic in describing transport in these ionomers.[2,3,7]

The equation for the impedance of the equivalent circuit in Figure 3 was presented earlier.[3] The real and imaginary components of the admittance ($Y^* = 1/Z^* = Y' + iY''$) are as follows:

$$Y' = R_2^{-1} + \omega^{1/2}/(2W) + Y_{ac}' \quad (1)$$

$$Y'' = \omega C_2 + \omega^{1/2}/(2W) + Y_{ac}'' \quad (2)$$

where

$$Y_{ac}' = \omega^2 C_1^2 R_1/q \quad (3)$$

$$Y_{ac}'' = \omega C_1/q \quad (4)$$

$$q = (\omega C_1 R_1)^2 + 1 \quad (5)$$

and $\omega = 2\pi f$, with f = the frequency of applied signal.

$1/R_2 = G_2$ is the "dc" conductance representing ion drift, *i.e.*, hopping over many contiguous clusters within the half-cycle during which the applied field is in the same direction at low f. A similar interpretation can be made of the term containing W, except that the directions between successive cluster-to-cluster hopping vectors are uncorrelated.

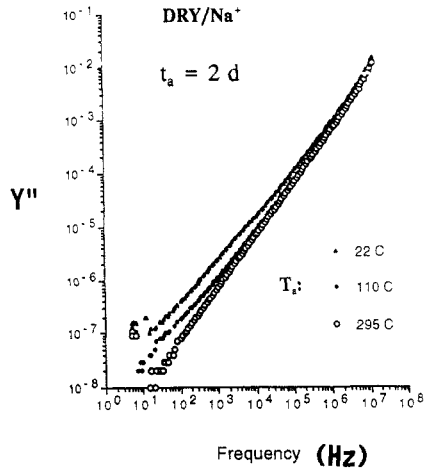

Figure 4. log–log plot of imaginary admittance (Y'', in Ω^{-1}) *vs* frequency (f) for dry Na^+-form PFSI membranes annealed 2 days at indicated temperatures T_a.

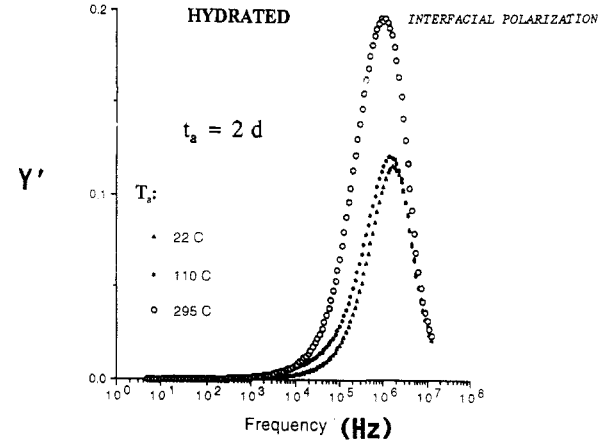

Figure 5. Y' (Ω^{-1}) *vs* log f for hydrated Na^+-form membranes previously annealed 2 days at indicated temperatures T_a.

The alternating accumulation ↔ dissipation of unbalanced charge at the cluster boundaries occurs with relaxation time $\tau = C_1R_1$ = time scale for intracluster motions.

If this model is valid, plots of either log Y' or log Y'' *vs* log f should be monotonically increasing in *linear* fashion at low frequencies with each exhibiting a superimposed *peak*, represented by Y_{ac}' or Y_{ac}'' according to eqs 3 and 4, at high f. The slope of the low-f log Y' *vs* log f line would be 0.500 for pure diffusion. The first term of eq 1 can be written as ω°/R_2, so that pure drift corresponds to a slope of 0.00. Hybrid drift–diffusion would produce a slope between 0.00 and 0.50. Migration pathways more tortuous than diffusion are represented by slopes >0.50. The low-f slope of log Y'' *vs* log f may be 1.00 or 0.500 or in between depending on the relative magnitudes of C_2 and W. Large C_2 favors slopes close to 1.00 (nonconductive grid). The peak should be more prominent for the Y' *vs* f curve than for the Y'' *vs* f curve.

Dry Membranes. The general features of eqs 1 and 2 are observed on experimental log Y' and log Y'' *vs* log f curves (not shown) for t_a = 2 days and T_a = 22, 110, and 295 °C.

The slope of the linear segment for the T_a = 295 °C Y' curve is ~0.80, suggesting numerous charge traps on the percolation grid. Equation 1 does not permit a value as high as 0.80, but we interpret the slope within a general fractal concept. Then this value is reasonable considering the difficulty of ion transport through *dry* membranes. There is a weak peak for T_a = 22 °C between 10^3 and 10^4 Hz, possibly related to *residual hydration* since it is absent at higher T_a. Drying of PFSI membranes is difficult and improves with increased T_a. If this relaxation is associated with intracluster ion motions, it would be enhanced with added water. Y' curves shift downward with increasing T_a, attributed to increasing R_2 with decreased hydration. If annealing enhances structural perfection and reduces free volume in the matrix, intercluster ion hopping becomes more difficult. An upswing in Y' at the highest frequencies at each T_a might be the wing of an off-scale peak whose relaxation time is somewhat longer than the rotational relaxation time of liquid water ($\tau \sim 10^{-11}$ s, or $f_{max} \sim 1.6 \times 10^{10}$ Hz[8,9]). Such a peak would lie only 2 orders of magnitude to the right of the highest accessible frequency. Ion–dipole interactions would slow tumbling motions to where the low-frequency wing is visible.

log Y'' *vs* log f plots (Figure 4) display linearity but no peak. The slope at low f indicates whether the ω- or the $\omega^{1/2}$-dependent term is dominant. The 295 °C curve displays greatest linearity over the broadest f range and greatest slope (1.0), indicative of hopping pathways more tortuous than those for pure diffusion although diffusion becomes more important with decreasing T_a as the slopes decrease. All curves merge at high f with common slope 1.0, indicating the membranes become very capacitive.

The implication of tortuous long-range ion motions and the fact that both Y' and Y'' plots exhibit the greatest linearity for the 295 °C case suggest that annealing at 295 °C induces considerable microstructural regularity. The increase in overall capacitance with increased T_a suggests tighter chain packing, giving rise to blocked intercluster ion hopping.

The downward shift of log ϵ' *vs* log f curves (not shown) with increasing T_a suggests overall polarizability diminishes with increasing T_a. Contrast between polarizabilities of the two phases would decrease with decreased residual hydration. A peak between 10^3 and 10^4 Hz is seen on log ϵ'' *vs* log f curves for T_a = 22 °C. Again, we identify this peak with interfacial polarization relaxation. As Na^+ mobility decreases and chain packing efficiency improves with drying–annealing, ϵ'' curves should be monotonically depressed over the frequency range, as is observed. An upswing in ϵ'' at the highest frequencies might, again, be the wing of a peak for which f_{max} decreases with increasing T_a. Given the mechanistic assignment of H_2O dipole rotation, longer relaxation times reflect increasing rotational restriction by ions.

Hydrated Membranes. Y' *vs* log f spectra of hydrated membranes, having very distinct high-frequency peaks (Figure 5), are dramatically different from the corresponding dry membrane spectra. The vertical scale of Figure 5 is considerably greater than those for the corresponding dry membranes, a consequence of the greater ionic conductivity of hydrated membranes. Y_{ac}' can be written as $G_1\{(\omega\tau)^2/[(\omega\tau)^2 + 1]\}$, where $G_1 = R_1^{-1}$ = *cluster conductance*, associated with Na^+ hopping *within* hydrated clusters, is the peak height in Figure 5. Figure 5 underscores the fact that the admittance representation accentuates relaxations in the high-frequency regime.

The peaks increase in height with increasing T_a. Since hydration capacity increases with increasing T_a, it is logical that the intensity of this peak, associated with interfacial polarization relaxation, is enhanced with increasing T_a. The difference in peak height/width between the 295 and 110 °C curves is much greater than the difference between the 110 and 22 °C curves. This ordering correlates with the ordering of the differences in water uptake, as well as differences in sharpness of the matrix glass transition.

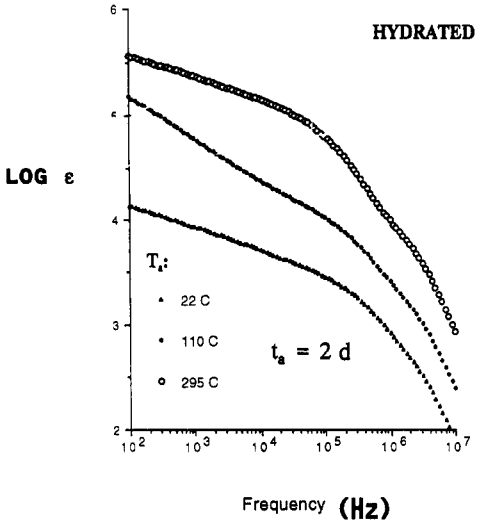

Figure 6. Same as in Figure 5, but for log ϵ'.

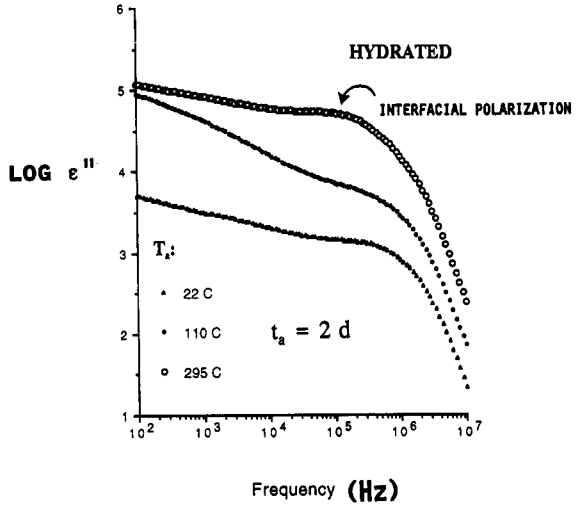

Figure 7. Same as in Figure 5, but for log ϵ''.

f_{max} progressively decreases with increasing T_a. This appears to contradict the notion that Na^+ mobility increases with increasing water content, which would cause the peak to shift to the right rather than the left. In addition to the intrinsic ion mobility, the fact that the *sizes* of the clusters increase with increased hydration is also significant. τ reflects the motional time scale for *cooperative* charge rearrangements over the entire cluster. These coupled aggregate motions become more sluggish (τ increases) as the cluster enlarges, accounting for the leftward peak shift. Theories relating to the dielectric response of similar heterogeneous systems predict this dependence of relaxation time on domain size.[10]

Corresponding Y'' *vs* log f curves (not shown) are displaced upward with increasing T_a. Curve sections to the left of the peak maxima for 22 and 110 °C are quite linear. Similar to Y' curves, peaks shift to lower f with increasing T_a with the same rationalization. There is an additional, inexplicable peak between 10^5 and 10^6 Hz for T_a = 295 °C. As for Y' peaks, the increase in Y'' peak height with increasing T_a is attributed to enhanced cluster conductance owing to augmented hydration.

Relaxation behavior from the permittivity perspective is shown in Figures 6 and 7. ϵ' curves progressively shift upward with increasing T_a, attributed to increasing hydration. When hydration increases, cluster volume fraction increases, which, in turn, increases not only Na^+ mobility but also the relative amount of polar/nonpolar interface. In this way, the magnitude of the interfacial polarization, directly reflected in ϵ', is enhanced. The vertical shifting of ϵ' curves for hydrated membranes with increasing T_a is the reverse of the shift for "dry" membranes. Also, values of ϵ' for hydrated membranes are considerably higher than the corresponding values for dry membranes, also due to a lower degree of interfacial polarization within dry membranes. An inflection on the log ϵ' *vs* log f curves for T_a = 295 °C somewhat below 10^6 Hz corresponds to a weak relaxation on the ϵ'' curve (Figure 7) at this temperature and frequency.

Upward vertical shifting with increasing T_a is seen for log ϵ'' *vs* log f curves, perhaps due to enhanced Na^+ transport (combination of decreasing R_2 and W) with hydration. A weak peak between 10^5 and 10^6 Hz for each T_a shifts to lower f with increasing T_a. It is again obvious that for highly conducting systems admittance is more effective in uncovering high-f relaxations while permittivity is more sensitive to the low-f phenomenon.

While semicircular vestiges are seen in the left (high f) portions of the Cole–Cole plots, monotonically increasing ϵ'' *vs* ϵ' behavior to the right of this feature reflects dominance of long-range ion transport. The radius of circles best fitted to high-f data increases with increasing T_a, presumably a manifestation of enhanced polarizability. The depression of the circle center beneath the ϵ' axis is quantified by $\alpha\pi/2$, the angle between the ϵ' axis and the circular radius intersecting this axis. α, the Cole–Cole distribution of relaxation times parameter,[12] becomes larger when the distribution broadens, reflective of microstructural heterogeneity. Since we have associated this relaxation with fluctuating interfacial polarization, an increase in α might be interpreted as an increase in distribution of cluster sizes or shapes.

α = 0.287, 0.245, and 0.144 for T_a = 22, 110, and 295 °C, respectively. The distribution of relaxation times becomes narrower with increasing T_a, especially for 295 °C. $T_{g,m}$ increases with increasing T_a, the transition being most profound and narrower for T_a = 295 °C. T_m also shifts upward with increasing T_a. Both amorphous and crystalline components of the matrix become more ordered with increasing T_a. These thermal trends correlate with the trend of decrease in α with increase in T_a. The environment surrounding clusters becomes more uniform with increasing T_a, contributing to a progressive decrease in α.

It is significant that $T_{g,c}$ is either absent or very weak for T_a = 295 °C on either first or second DSC scan. It was suggested that if the membrane is annealed above $T_{g,c}$ and then rapidly cooled, disorder is frozen into the packing of side chains. On the other hand, there would also be more thermal inducement for side chains that exist in isolation or in small aggregates to be added to existing clusters and thereby cause clusters to grow in size. The latter rearrangement would narrow the distribution of cluster sizes as small side chain aggregates are removed from the ensemble to contribute to a decrease in α.

Variation of Time of Annealing (t_a; T_a = 295 °C). Differential Scanning Calorimetry. DSC scans for T_a = 295 °C for t_a = 1–48 h (40 °C/min) show a trend in $T_{g,m}$ (inflection point temperature) in Table 2. Save for t_a = 48 h, $T_{g,m}$ increases with increasing t_a. This is logical considering that longer times at high temperature allow more motional opportunities for chains to improve packing efficiency, although the 48-h scan is ubiquitous. Second scans—again, having rapidly cooled with ice from the maximum temperature attained during first scans (~200 °C)—show no evidence for a matrix glass transition, at least at temperatures observed for unannealed membranes.

Table 2. Matrix Glass Transition Temperature ($T_{g,m}$, °C) vs Time of Annealing (t_a, h) for Dry Na^+-Form 803 EW PFSI Membranes[a]

t_a	$T_{g,m}$	t_a	$T_{g,m}$
1	143	22	156
3	152	48	151
12	154		

[a] T_a = 295 °C. Data for first scan. Heating rate is 40 °C/min.

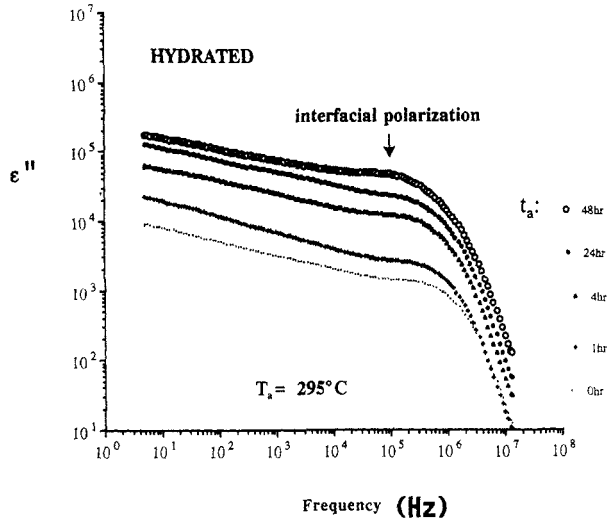

Figure 8. log ϵ'' *vs* log f for hydrated membranes, T_a = 295 °C, for indicated t_a.

The matrix glass transition also disappeared on second scans for t_a = 2 days for different T_as. Furthermore, the cluster glass transition for both first and second scans at t_a = 2 days disappears for T_a = 295 °C. There is no evidence of an ionic cluster glass transition in second scans for the t_a studies at 295 °C.

There is an endotherm in second scans initiated at 210–220 °C that shifts to lower temperatures with increasing t_a. This does not seem to be the matrix glass transition whose temperature increased as a result of the first scan. If matrix molecular structure is indeed refined with increased t_a, the transition would move to higher, not lower, temperatures. Furthermore, perfection of matrix crystallinity reflected by a more pronounced melting endotherm is not seen in second scans. Perhaps annealing at 295 °C followed by cooling after the first scan freezes disorder in the matrix so that an order → disorder transition is suppressed upon reheating.

It was earlier suggested that annealing at 295 °C for 2 days followed by cooling erases the ionic cluster glass transition. Perhaps this process causes $T_{g,c}$ to shift downward with increasing t_a for shorter times with gradual diminution of intensity. This would account for the endotherm discussed above, as this behavior is in fact observed.

Dielectric Relaxation. log ϵ'' *vs* log f curves for *dry* membranes, T_a = 295 °C, are monotonically depressed as t_a advances from 0 to 48 h, due, presumably, to progressively lower residual hydration. An off-scale peak for all curves appears with $f_{max} > 10^7$ Hz, decreasing with increasing t_a. This feature also shifts to lower f with increasing T_a for t_a = 2 days. Furthermore, a low-frequency peak, between 10^3 and 10^4 Hz, exists for the shortest t_as. This peak was also seen for T_a = 22 °C, t_a = 2 days.

log ϵ'' *vs* log f curves for the corresponding *hydrated* membranes are in Figure 8. Although there is a hint of a peak between 10^5 and 10^6 Hz, all spectra are overwhelmed by the manifestation of long-range ion transport. The left-hand sections of all curves are very linear, the domain of linearity decreasing with increasing t_a. The lines have slopes $n \approx 0.20$, the low value reflecting very tortuous ion-hopping pathways, a result that is surprising, considering the high degree of hydration.

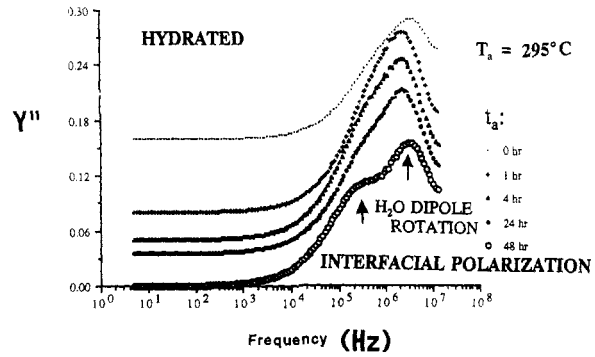

Figure 9. Same as for Figure 8, but for Y''.

While the curves in Figure 8 are separated vertically to view them more distinctly, as they greatly overlap, the actual ordering is such that the curves do shift upward with increasing t_a. This is ascribed to increase in hydration with increasing t_a: Increased hydration enhances long-range Na^+ mobility, allowing ions to execute greater displacements during half-cycles of the applied signal. G_2 increases with increasing hydration. The order of vertical curve displacement in Figure 8 is the reverse of that for dry membranes.

Loss peak maxima in Figure 8 shift to lower f with increasing t_a, similar to the leftward shift of this peak with increasing T_a at constant t_a. We rationalize there will be an increase in cluster size with increased hydration caused by longer annealing; larger clusters have longer relaxation times associated with the coupled motions of ions and water molecules therein.

The relaxation between 10^5 and 10^6 Hz in Figure 8 appears as a peak in the corresponding Y'' *vs* log f spectra (Figure 9) which shifts to lower f and evolves into an increasingly stronger shoulder on a more prominant peak with increasing t_a. The major peak remains at ~2 MHz for t_a = 1, 4, and 24 h and shifts to ~3 MHz for t_a = 48 h. The 0-h peak also occurs at ~3 MHz. The coexistence of two peaks whose f_{max} differ by only about an order of magnitude is rationalized as follows.

The opposite shifting of these two peaks with hydration conflicts with an earlier view[2,3] that two peaks in close proximity reflect the same relaxation but for clusters differing in size. We believe the low-f peak is the major process regardless of hydration since interfacial polarization relaxation is more profound than molecular dipole rotation.[13] f_{max} for interfacial polarization does in fact decrease with increased hydration (*i.e.*, increasing T_a at fixed t_a or longer t_a at fixed T_a) as, in fact, is observed for the lower f component for this system.

While the high-f peak mechanism is unidentified, consider a Debye-like H_2O dipole reorientation for cluster-contained molecules. Figure 10 contains the corresponding Y' *vs* log f plots for hydrated membranes. Each single peak maximum lies at a frequency between those of the two peaks in the Y'' plots in Figure 9. The Y'' counterpart of this Y' peak is the low-f component since both peaks shift to lower f with increasing t_a. Perhaps a high-f peak also exists on Y' plots but beyond the upper measurement limit. It does not appear that the peaks in Figure 10 are superpositions of two peaks.

Although the curves in Figure 10 are artificially vertically separated for visual discrimination, peak heights in

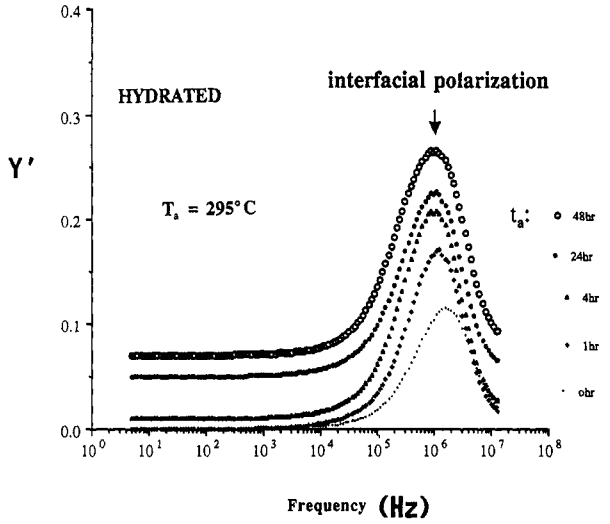

Figure 10. Same as for Figure 9, but for Y'.

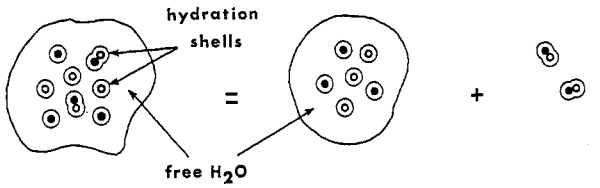

Figure 11. Partitioning of cluster "nanosolution" into free (H-bonded) *vs* ion-bound H_2O molecules and dissociated ions *vs* contact ion pairs.

untouched plots increase with increasing t_a and $Y' \rightarrow 0$ as $f \rightarrow 0$ (relative to scale) for all curves. Increasing peak height corresponds to increasing G_1, which is related to enhanced *intra*cluster Na^+ mobility with increased hydration. Increased G_1 might at first be thought to shorten interfacial polarization relaxation time, causing the peak to shift rightward; the peak in fact shifts to the left. We believe that the *cooperative* motions of all ions and H_2O molecules in clusters is more profound than single-ion intracluster mobility in controlling relaxation time; the more water molecules/cluster, the more sluggish is the coupled motion.

Assume the high-f Y'' peak in Figure 9 is associated with H_2O dipole reorientation within clusters. These rotations are restricted by hydrogen bonding and ion–dipole interactions. "*Nanosolutions*" as such contrast sharply with bulk electrolytes in possessing extremely large surface/volume. Of all H_2O molecules in a cluster, a considerable fraction resides at the surface so that when hydration increases, there is a large *relative* decrease in this surface fraction. If clusters are approximately spherical, their surface/volume is inversely proportional to radius. When clusters become more hydrated, the overall degree of hydrogen bonding increases and the average H_2O molecule has more like molecules coordinated about it.

Water molecules in PFSI clusters can be ion-bound or liquidlike (Figure 11).[15,16] Average H_2O dipole rotational mobility increases with increasing hydration (f_{max} increases) in the same way that H_2O dipole reorientation time in bulk electrolytes increases with increasing ion concentration.[17] Perhaps this rationale can be applied to the high-f peak shift in Figure 9 from t_a = 1 to 48 h as well as to the leftward shift of the high-f ϵ'' peak with increasing t_a for "dry" membranes. As t_a progresses from 1 to 24 h, little shifting of the high-f Y'' peak occurs (Figure 9). Perhaps the immediate environment about the average H_2O molecule remains rather constant at these hydration levels, but at 48 h H_2O rotational mobility increases since

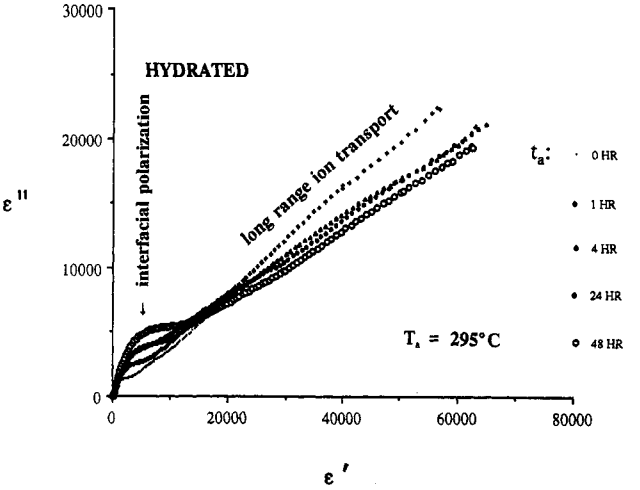

Figure 12. Cole–Cole plots for T_a = 295 °C for indicated t_a and then hydrated.

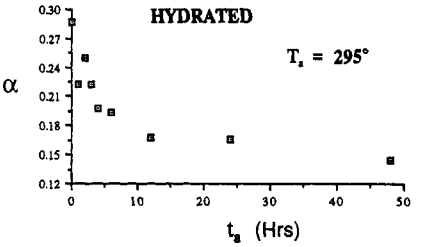

Figure 13. Distribution of relaxation time parameter (α), T_a = 295 °C, as a function of t_a and then hydrated.

f_{max} increases. Resulting from annealing for this considerable time > $T_{g,c}$, clusters became disordered so that side chains pack considerably more loosely. If cluster free volume thereby increases drastically as t_a jumps from 24 to 48 h, the number of H_2O molecules in clusters will increase significantly, producing a more liquidlike state and faster dipole relaxation.

Cole–Cole plots for hydrated membranes as a function of t_a, T_a = 295 °C, are shown in Figure 12. The high-f arcs at the left correspond to interfacial polarization relaxation. The linear sections on the right are due to long-range ion transport. The slope of the t_a = 1 h line is greater than those for the other t_as, all of which are essentially the same. It was earlier established that $\epsilon'' \sim f^{-n}$ for these systems in the low-f regime. The exponent n is related to the slope of the linear segment on the Cole–Cole plot by[18]

$$\text{slope} = \tan(n\pi/2) \tag{6}$$

Using eq 6, n = 0.18 for t_a = 48 h, which is rather low considering that this membrane has the greatest hydration, although chain packing in the matrix may be so efficient that ions have difficulty hopping *between* clusters while intracluster ion motions are rather facile. n = 0.23 for t_a = 1 h, the case for which the ϵ'' *vs* ϵ' slope is greatest: ion-hopping pathways are still more tortuous than random.

The distribution of relaxation times parameter for semicircles fitted to the arcs is plotted *vs* t_a in Figure 13. α significantly decreases with increasing t_a, indicating distribution narrowing, in turn suggesting the distribution of cluster structure or perhaps structure around clusters narrows.

The proposed Debye-like water dipole relaxation in clusters does not appear in Figure 12, but a magnification of these plots about the origin reveals tails trailing from the high-f sides of the arcs.

Conclusions

Dry, short side chain Na^+-PFSI membranes were annealed at 22, 110, and 295 °C for varying times. Annealing-induced microstructural reorganizations in either matrix or cluster phases were monitored by DSC. The matrix glass transition is most profound for T_a = 295 °C > $T_{g,c}$ in first-scan traces, but disappears in the second scan after the first-scan sample is rapidly cooled from a temperature between $T_{g,m}$ and $T_{g,c}$. T_m also increases with increasing T_a. Annealing at this temperature above $T_{g,c}$ results in increased order and more structural cohesion in the matrix. The ionic cluster transition, present for T_a = 22 and 110 °C, disappears for T_a = 295 °C in both first and second scans. Annealing above $T_{g,c}$ induces the most significant structural changes.

Hydrative capacity increases with increasing T_a at constant t_a, which was rationalized in terms of increased disorder in side chain packing resulting in greater free volume in clusters. Heaney *et al.* conducted a morphological investigation of heat-treated short side chain, Na^+-form PFSIs using SAXS.[19] While the membranes of Heaney *et al.* were heated in glycerin whereas ours were first annealed and then hydrated, it is interesting that these investigators found that ionic cluster size increases with increasing maximum temperature used during treatment. We suggest that the increase in solvated cluster size with increasing temperature observed in their studies is due at least in part to our proposed annealing mechanism assisted by structural plasticization by glycerin. Heaney and Pellegrino determined by SAXS that the size of ionic clusters in Na^+-form 1100 EW Nafion, glycerol-imbibed membranes increases monotonically with temperature.[20] Gierke used the SAXS "cluster" peak for long side chain membranes to determine the manner in which cluster diameter increased with water content.[21] Moore and Martin, as a result of a SAXS study of short side chain membranes, concluded that cluster size increases with increasing hydration.[4]

Electrical impedance studies were performed over a broad frequency range at room temperature on dry and hydrated membranes that were annealed as described above. The permittivity representation is most useful for studying long-range ion transport at low frequencies while admittance is better suited for detecting cluster-confined ion and (postulated) H_2O dipole motions at high frequencies.

Shifts of peak intensities and relaxation times with T_a and t_a for intracluster motions were rationalized in terms of changes in water structure. The peak associated with interfacial polarization relaxation was rationalized as shifting to lower f with increase in either T_a or t_a on the basis of increase in hydrated cluster size. We suggest that annealing increases the hydrative capacity of clusters. As clusters increase in size, cooperative motions within them become more sluggish. It was also suggested that a peak appearing at higher frequencies is associated with the relaxation of H_2O dipoles in hydrated clusters. An analysis of the Cole–Cole distribution of relaxation times parameter indicates that annealing at 295 °C induces considerable microstructural regularity.

Analyses of low-f spectral regions for both dry and hydrated membranes suggest that annealing generates rather tortuous ion-hopping pathways, in harmony with the idea that free volume in intercluster regions shrinks with annealing.

These studies suggest that while side chain packing becomes disordered, the matrix becomes more homogeneous and more tightly packed with increasing T_a at constant t_a or with increasing t_a at constant T_a. As degree of order in one phase is increased, order in the other is correspondingly disrupted in coupled fashion.

Acknowledgment. The authors gratefully acknowledge the support of the Dow Chemical Co. for this work.

References and Notes

(1) *Perfluorinated Ionomer Membranes*; Eisenberg, A., Yeager, H. L., Eds. ACS Symposium Series 180; American Chemical Society: Washington, DC, 1982.
(2) Deng, Z. D.; Mauritz, K. A. *Macromolecules* **1992**, *25*, 2739.
(3) Deng, Z. D.; Mauritz, K. A. *Macromolecules* **1992**, *25*, 2369.
(4) Moore, R. B.; Martin, C. R. *Macromolecules* **1989**, *22*, 3594.
(5) Tant, M. R.; Darst, K. P.; Lee, K. D.; Martin, C. W. In *Multiphase Polymers: Blends and Ionomers*, Utracki, L. A., Weiss, R. A., Eds.; ACS Symposium Series 395; American Chemical Society: Washington, DC, 1989; Chapter 15.
(6) Numerous examples are within the following: MacDonald, J. R. *Impedance Spectroscopy*; Wiley-Interscience: New York, 1987.
(7) See the following and references contained therein: Mauritz, K. A. *Macromolecules* **1989**, *22*, 4483.
(8) Lane, J. A.; Saxton, J. A. *Proc. R. Soc. London, Ser. A* **1952**, *213*, 400.
(9) Brot, C.; Magat, M.; Reinisch, L. *Kolloid-Z.* **1953**, *134*, 101.
(10) (a) If the mobile ions lie near the surface of a cluster, then $\tau \propto$ cluster surface area. A theory by Schwartz was developed for suspended colloidal particles but is mathematically equivalent to a treatment of ionic clusters in ionomers with secondary modifications. Schwartz, G. *J. Phys. Chem.* **1962**, *66*, 2636. (b) If the mobile ions are distributed throughout the entire volume of a cluster, then $\tau \propto$ cluster volume. A theory by Oosawa was developed for charged polyelectrolyte coils in aqueous solutions that is mathematically equivalent to a treatment of ionic clusters in ionomers with secondary modifications. Oosawa, F. *Polyelectrolytes*; Marcel Dekker: New York, 1971.
(11) Starzak, M. E. *The Physical Chemistry of Membranes*; Academic Press: Orlando, 1984; p 158.
(12) Cole, K. S.; Cole, R. H. *J. Chem. Phys.* **1941**, *9*, 341.
(13) Mauritz, K. A.; Fu, Ruey-Mei *Macromolecules* **1988**, *21*, 1324.
(14) Debye, P. *Polar Molecules*; Chemical Catalogue Co.: New York, 1929.
(15) Komoroski, R. A.; Mauritz, K. A. In *Perfluorinated Ionomer Membranes*; Eisenberg, A., Yeager, H. L., Eds.; ACS Symposium Series 180; American Chemical Society: Washington, DC, 1982; p 113.
(16) Mauritz, K. A.; Gray, C. L. *Macromolecules* **1983**, *16*, 1279.
(17) (a) Lane, J. A.; Saxton, J. A. *Proc. R. Soc. London, Ser. A* **1952**, *213*, 400. (b) Brot, C.; Magat, M.; Reinisch, L. *Kolloid-Z.* **1953**, *134*, 101.
(18) Su, Shunfua, Ph.D. Dissertation, An Investigation of Long and Short Range Ion Motions within the Cluster Morphology of Electrolyte-Containing Perfluorosulfonate Ionomer Membranes; University of Southern Mississippi, 1992.
(19) Heaney, M. D.; Glugla, P. G.; Martin, C. W.; Harthcock, M. A. 33rd IUPAC International Symposium on Macromolecules, Montreal, 1990, *Book of Abstracts*, Session 1.3.8.
(20) Heaney, M. D.; Pellegrino, J. *J. Membr. Sci.* **1989**, *47*, 143.
(21) Gierke, T. D.; Munn, G. E.; Wilson, F. C. *J. Polym. Sci., Polym. Phys. Ed.* **1981**, *19*, 1687.